

Online and offline tools for head movement compensation in MEG

Arjen Stolk^{a*}, Ana Todorovic^a, Jan-Mathijs Schoffelen^{a,b}, Robert Oostenveld^a

^aRadboud University Nijmegen, Donders Institute for Brain, Cognition and Behaviour;

^bMax Planck Institute for Psycholinguistics, Nijmegen, Netherlands,

* arjen.stolk@donders.ru.nl

Abstract

Magnetoencephalography (MEG) is measured above the head, which makes it sensitive to variations of the head position with respect to the sensors. Head movements blur the topography of the neuronal sources of the MEG signal, increase localization errors, and reduce statistical sensitivity. Here we describe two novel and readily applicable methods that compensate for the detrimental effects of head motion on the statistical sensitivity of MEG experiments. First, we introduce an online procedure that continuously monitors head position. Second, we describe an offline analysis method that takes into account the head position time-series. We quantify the performance of these methods in the context of three different experimental settings, involving somatosensory, visual and auditory stimuli, assessing both individual and group-level statistics. The online head localization procedure allowed for optimal repositioning of the subjects over multiple sessions, resulting in a 28% reduction of the variance in dipole position and an improvement of up to 15% in statistical sensitivity. Offline incorporation of the head position time-series into the general linear model resulted in improvements of group-level statistical sensitivity between 15% and 29%. These tools can substantially reduce the influence of head movement within and between sessions, increasing the sensitivity of many cognitive neuroscience experiments.

Key words: magnetoencephalography, real-time head localization, general linear modeling, regression analysis

1. Introduction

MEG measurements are performed with superconductive magnetic field sensors that are mounted inside a helmet-shaped dewar. The subject's head is positioned under the dewar as close as possible to the sensors, but in most MEG experiment settings the subject's head is not fixated. The consequence is that the subject's head, and thereby the neuronal sources in the brain generating the neuromagnetic fields, can move relative to the MEG sensors. To minimize the detrimental effects of head movements on the data, subjects are typically instructed by the experimenter to maintain the same posture and lay or sit still throughout the recording, which can take a considerable amount of time.

Head movement during recording causes topographical blurring of the measurements at the sensor level and thereby introduces source localization errors ([Medvedovsky et al., 2007](#); [Uutela et al., 2001](#)). Also, the mixture of different head positions over time adds variance to the data that is not accounted for by the experimental manipulation, thus potentially deteriorating statistical sensitivity. Studies that involve subjects who have difficulty remaining still ([Gaetz et al., 2008](#); [Wehner et al., 2008](#)) or studies that involve recordings of the same subject in multiple sessions (potentially over multiple days) ([Nieuwenhuis et al., 2008](#)), face a related problem. A difference in the head position causes not only the MEG sensor level topographies to be inconsistent between the sessions, but may also lead to differences in the signal-to-noise ratio between sessions, due to the weaker signal that is picked up from a source when it is further away. Without accurate repositioning over sessions, the comparison or the combination of data from separately recorded sessions suffers from the increased between-sessions variance.

Ideally, one would allow the MEG subjects to move freely and correct the sensor level data for the movements. In EEG recordings, head movements are in principle not problematic because the electrodes move along with the head. For fMRI it is possible to compensate for movements during the acquisition by instantaneous adjustments of the gradients ([Maclaren et al., 2012](#); [Thesen et al., 2000](#)). Future advances with optically pumped magnetometers ([Kominis et al., 2003](#); [Sander et al., 2012](#)) may result in a cap-style MEG sensor array that can move along with the head. At present, MEG recordings have to be performed with a spatially fixed sensor array, relative to which the head can move. Offline compensation methods are available to correct the raw sensor level data ([Knosche, 2002](#); [Numminen et al., 1995](#); [Taulu et al., 2005](#); [Uutela et al., 2001](#)), which attempt to approximate the MEG data that would have been recorded, had the head been on a fixed position relative to the sensors. The compensation techniques rely on model assumptions, such as stationarity of the signal-to-noise ratio and the field distributions. However, after correction the MEG data does not correspond ideally with the desired data due to the imperfection of the assumptions and the difficulty for the user selecting the optimal algorithm parameters.

Preferably, head position differences and movements are avoided in the first place, e.g. by fixating the subject's head using a subject specific nylon or silicon head-cast (Gareth Barnes, personal communication). Bite-bars have been employed in MEG for the purpose of accurate co-registration with MRI ([Adjamian et al., 2004](#); [Singh et al., 1997](#)) but have not been used to fixate the head relative to the MEG sensors. For magnetic resonance imaging bite-bars have sporadically been used to reduce head movements (e.g. ([Heim et al., 2006](#))). However, a limiting factor in the applicability of a

bite-bar in MEG recordings is increased muscle tension in the jaw muscles and the associated increase in noise.

Besides implementing strategies to avoid head movements, methodological advances in the past decade have been proposed to compensate for the effects of head movements in offline data analysis. For this purpose, most MEG systems are able to continuously localize the position of the head relative to the dewar ([de Munck et al., 2001](#); [Uutela et al., 2001](#); [Wilson, 2004](#)). Yet, the majority of published MEG studies to date do not incorporate this knowledge about head movements in the analysis pipelines. The present study explores the potential of using continuous head location monitoring for online and offline head movement compensation with a focus on the consequences of head movements on statistical sensitivity. Without downplaying the relevance of obtaining crisp MEG sensor-level topographies and accurate source localizations, most cognitive research questions are addressed using an experimental manipulation to statistically test a hypothesis. Consequently, the effects of head movements have impact on the usability and sensitivity of MEG in the study of cognition.

The remainder of the introduction is structured as follows: We will first provide a common methodological framework that describes the problem of variability in head position. Subsequently, we will present each of the existing methods suggested in the literature in this common framework and explain their opportunities and limitations. Finally, we will introduce our methodological contributions and how we will assess their potential for improving statistical sensitivity.

For a given source \mathbf{S} with location r and time sample t , the data \mathbf{X} at MEG sensors can be represented as the magnetic field of that source projected through lead field \mathbf{L} (i.e. the physical forward model of the field distribution):

$$\mathbf{X}(t) = \mathbf{L}(r) \cdot \mathbf{S}(r, t) + \mathbf{N}(t) \quad (1)$$

where \mathbf{N} is measurement noise. The dimensions of matrix \mathbf{X} and \mathbf{N} are channels by time samples, the dimensions of matrix \mathbf{L} are channels by number of source components (e.g. three orientations for a free-orientation dipole), and the dimensions of matrix \mathbf{S} are number of source components by time samples. Rather than expressing the position of the head relative to the sensors, we consider the position of the MEG sensors relative to the head and the location r of the source is also expressed relative to the head. If we now consider that the MEG sensors move relatively to the head, the data can be described as

$$\mathbf{X}(t) = \mathbf{L}(r_s; r_h) \cdot \mathbf{S}(r_s, t) + \mathbf{N}(t) \quad (2)$$

where r_s is the source location and r_h is the helmet location, i.e. the position of the helmet-shaped sensor array relative to the head. When r_h is not constant over time samples t , such as after head movements within a recording session or after the concatenation of separate sessions, this will introduce variability over time of \mathbf{L} and thereby of the signal in data \mathbf{X} . In terms of MEG experiments involving repeated trials of an evoked or induced brain response, different head positions will cause trial-by-trial variance that is not accounted for by the description of the experimental manipulation. Consequently, this leads to blurred topographies, increased localization errors, and reduced statistical sensitivity.

The existing offline approaches that try to compensate for head movements can broadly be divided into two categories. One category accounts for head position

differences and movements at the sensor level and the other category at the source level. The sensor level correction is based on the interpolation/extrapolation, or realignment, of the magnetic field distribution measured by the sensor array to a magnetic field distribution that would have been measured had the sensors been at the desired location. This interpolation can be achieved by an inverse modeling step, based on a distributed source model and using the original sensor positions, followed by a forward modeling step, where the reconstructed source activation is projected to a new set of sensor positions ([Knosche, 2002](#); [Numminen et al., 1995](#)) (see Eq. (7)). Typically, the inverse model involves a regularized minimum norm estimate, using a large number of dipoles that are placed near the surface of the brain compartment. Another approach is signal space separation (SSS), which allows for a sensor level interpolation that is based on modeling the magnetic field distribution using a set of spherical harmonic functions ([Medvedovsky et al., 2007](#); [Taulu et al., 2005](#)). The model can subsequently be used to estimate the magnetic field distribution at the desired sensor positions. This technique is implemented in the ‘MaxFilter’ software (Elekta Neuromag Oy, Helsinki, Finland).

Alternatively, head position information can be incorporated into the source reconstruction procedure. Source reconstruction involves the construction of an inverse linear operator, that can be thought of as a (pseudo-) inverse of the lead field, \mathbf{L}^+ ([Dale and Sereno, 1993](#)). Typically, the lead field matrix and its inverse are considered to be time-invariant, assuming a fixed position of the neuronal source model with respect to the sensors. Variability of the positions of the MEG sensors relative to the head can be taken into account by adjusting the lead field gains that relate the source amplitudes to the field

distribution ([Uutela et al., 2001](#)). Correspondingly, the estimated source activity $\hat{\mathbf{S}}$ can be expressed as:

$$\hat{\mathbf{S}}(r_s, t) = \mathbf{L}^+(r_s; r_h) \cdot \mathbf{X}(t) \quad (3)$$

where r_h reflects the position of the MEG sensors relative to the head. The lead field matrix can be adjusted on a trial-by-trial basis, i.e. by using a separate lead field for each trial/repetition k corresponding to the head position during that trial, and by averaging afterwards:

$$\hat{\mathbf{S}}_{avg}(r_s, t) = \frac{1}{K} \sum_{k=1}^K \mathbf{L}_k^+(r_s; r_{h,k}) \cdot \mathbf{X}_k(t) \quad (4)$$

Alternatively, information about the head positions during the recording is first averaged over repetitions and then represented in a spatially blurred version of the lead field:

$$\mathbf{L}_{avg} = \frac{1}{K} \sum_{k=1}^K \mathbf{L}_k(r_s; r_{h,k}) \quad (5)$$

Inversion of this trial-averaged lead field, in combination with the trial-averaged data, leads to the forward calculation corrected estimate:

$$\hat{\mathbf{S}}_{avg}(r_s, t) = \mathbf{L}_{avg}^+ \cdot \frac{1}{K} \sum_{k=1}^K \mathbf{X}_k(t) \quad (6)$$

The implementation according to Eq. (6) has been shown to be significantly less noise-sensitive than Eq. (4) ([Uutela et al., 2001](#)) because the inverse operator is typically obtained using a regularization of the lead field \mathbf{L} with an estimate of the noise covariance, which can be more robustly estimated across multiple trials compared to on a single trial level (see also ([Dale and Sereno, 1993](#))).

Note that when estimation of the source amplitude is followed by a forward modeling step towards a new set of sensor positions r_o , the realigned magnetic field

distribution \mathbf{X}_0 as described above ([Knosche, 2002](#); [Numminen et al., 1995](#)) can be obtained:

$$\mathbf{X}_0(t) = \mathbf{L}(r_s; r_0) \cdot \hat{\mathbf{S}}(r_s, t) \quad (7)$$

where \mathbf{X}_0 can be either estimated per trial using $\hat{\mathbf{S}}_k$ or for the average using $\hat{\mathbf{S}}_{avg}$. The SSS-based MaxFilter method ([Taulu et al., 2005](#)) is conceptually comparable to this, except that it uses lead fields based on a harmonic expansion of the magnetic field in the volume of the sensor array rather than lead fields based on a neurophysiologically inspired dipole source model.

The methods described above can only approximate (i.e. inter-/extrapolate) the data that would have been measured if there had been no head movements, to the level that the assumptions of those methods (e.g. field distributions and stationarity of the signal-to-noise) are met. Furthermore, these methods are all relatively complicated modeling approaches that need detailed additional information and choices to be made, such as geometric information with respect to the source and volume conduction model when using an inverse/forward modeling approach, the selection of cut-off values in the regularization of the lead field inversion ([Hamalainen and Ilmoniemi, 1994](#)), or the number of expansion coefficients when using spherical harmonic functions ([Nurminen et al., 2008](#); [Taulu et al., 2005](#)). As a consequence, these methods are not guaranteed to work robustly in a wide variety of experimental situations.

Here we introduce and quantify the performance of head movement compensation techniques that are not based on sensor interpolation or lead field adjustments. Crucially, we demonstrate that the proposed tools can be readily applied to a wide range of tasks and experiments. First, we test a real-time head localizer that provides continuous visual

feedback about the subject's current head position; both to the experimenter and to the subject (see section 2.5 and 2.7). This allows for accurate online repositioning of the head between separate recordings, reducing the between-sessions variance. Second, we use general linear modeling (GLM; see section 2.8) to remove head movement related trial-by-trial variance from the data ([Worsley and Friston, 1995](#)), both at the sensor- and source level. By incorporating time-varying head position in the data analysis, the GLM allows to reduce the effect of movements.

We study the application of these two techniques in MEG experiments with various tasks covering different sensory modalities. We assess the consequences to the variance in the position of a dipole fitted to somatosensory evoked fields ([Haegens et al., 2010](#); [Litvak et al., 2007](#); [Medvedovsky et al., 2007](#)) and to the t-statistics of source-reconstructed ('beamformed') visually induced gamma-band activity ([Hoogenboom et al., 2006](#)) and ('minimum-norm estimated') auditory evoked fields ([Todorovic et al., 2011](#)). For validation, we test the performance of the offline GLM method on data from three large MEG group studies.

2. Methods

The data for this study comprises two parts. For the first part we use MEG recordings to investigate the performance for single subject data. These recordings were performed specifically to test the online head repositioning method and as a proof of principle for the offline GLM method. For the second part we address the performance of the offline GLM method for group analysis, using MEG data from three previously performed group MEG studies.

2.1. Subjects

For the single subject analyses, two subjects, *MN*; male, aged 29, *LB*; female, aged 25, took part in this study. They had no history of psychiatric or neurological problems and had normal (*LB*) or corrected-to-normal (*MN*) vision. Both subjects gave informed consent according to institutional guidelines of the local ethics committee (CMO Arnhem-Nijmegen, The Netherlands).

For the group analyses, we used MEG datasets obtained from studies performed by colleagues and that contained similar experimental stimuli as those used in the single subject recordings. The first dataset ($N = 16$) originated from a group study on somatosensory spatial attention ([Haegens et al., 2012](#)). The second dataset ($N = 32$) was taken from a study investigating the genetic determination of visually induced gamma-band peak frequency ([van Pelt et al., 2012](#)). A study on neuronal suppression in auditory cortex ([Todorovic and de Lange, 2012](#)) provided us with the third dataset ($N = 20$).

2.2. Experimental design and procedures

We here first describe the single subject experimental paradigm. To test whether repositioning of the subject's head using a real-time head localizer (see section 2.5)

improves the consistency and statistical sensitivity of the data, we recorded and analyzed two pairs of measurements (see Fig. 1), totaling four experimental recording sessions labeled A, B, C and D. Each session was started by positioning the subject in the MEG scanner. At the beginning of session A the subject was placed comfortably in the scanner. At the beginning of session B the subject was repositioned to session A. At the beginning of session C the subject was not repositioned, but again placed comfortably in the scanner. At the beginning of session D the subject was repositioned to session B. One measurement pair comprises data recorded in sessions B and D ('dataset BD'; with repositioning), another that of sessions A and C ('dataset AC'; without repositioning). We evaluated the consistencies in task-specific effects evoked during three tasks each involving a different sensory modality (see section 2.3). The specific tasks were selected for their wide coverage and relevance in recent cognitive research questions and serve to demonstrate the applicability of the investigated techniques to a wide range of tasks and experiments.

Subjects visited the laboratory on two separate days, taking part in four sessions in total (see Fig. 1). Each session involved the three tasks explained below (see section 2.3). The first two sessions (sessions A and B) were recorded on day I, the other sessions (sessions C and D) were recorded at a similar time on day II (Fig. 1). By recording the sessions on two separate days, we reduce the differences in evoked and induced responses due to fatigue and other time-specific effects. Subject *MN* re-visited the lab two weeks after the first session and subject *LB* re-visited the lab on the subsequent day. Within each session the subjects were instructed to maintain the same head posture during the three consecutive tasks. This instruction was identical to the normal

procedures in our MEG lab. The subjects were not informed about the purpose of the study regarding the head movements, but were debriefed following the last session. To keep the subjects naive with respect to the reason of leaving the scanner prior to session B on day I and D on day II, they were instructed to perform a reading test outside the scanner in which they had to pronounce 50 English words as quickly as possible (~1 min, *MN*; 59 and 49 s, *LB*; 64 and 54 s).

The group MEG studies each involved a specifically designed experimental paradigm addressing the respective cognitive research question. Detailed descriptions of the experimental paradigms can be found elsewhere ([Haegens et al., 2012](#); [Todorovic and de Lange, 2012](#); [van Pelt et al., 2012](#))

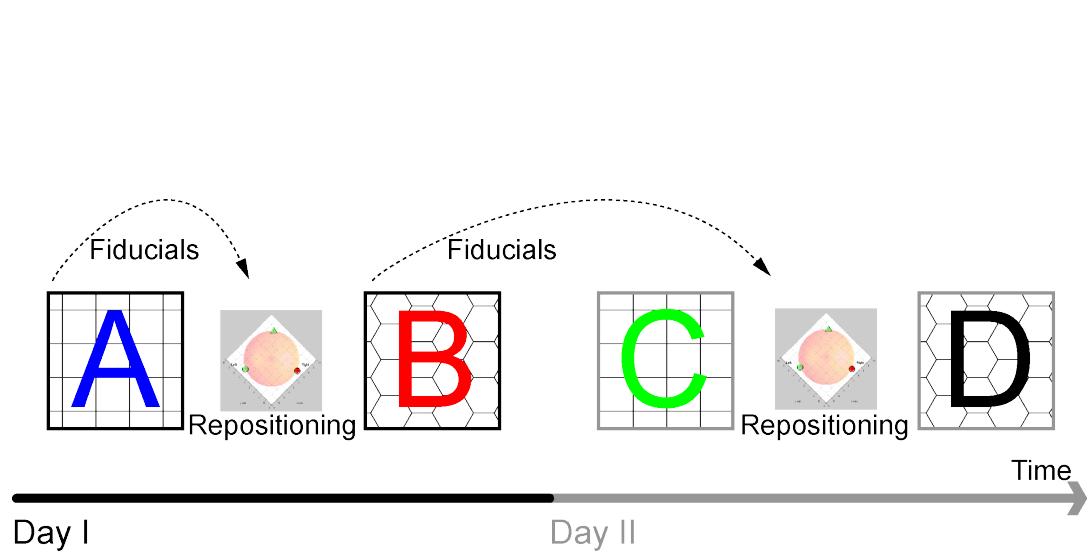


Fig. 1. Experimental design. Subjects' head positions and task-induced brain activity were recorded during four sessions (A, B, C, and D) on two separate days. Prior to recording session B on day I, subjects repositioned their heads to their initial position of session A using a real-time head localizer that displayed the real-time fiducial locations in 3-D. On day II, repositioning was done prior to the second session of that day (session D). The target fiducial locations for session D were the initial locations obtained from session B. The analyses focused on the combinations of recordings during sessions B and D (with repositioning) and on those of sessions A and C (without).

2.3. Materials

A single MEG session (~30 min) of a single subject recording consisted of three consecutive tasks involving different sensory modalities. In each task, a small fixation cross was presented in the center of the projection screen during stimulus presentation and inter-stimulus intervals (ISI). Subjects were instructed to fixate on this cross to reduce ocular activity. Trials were interspersed with occasional blank periods when the subjects were encouraged to blink.

In the first task (tactile task, ~10 min), subjects' median nerves were stimulated by applying an electrical pulse to the left index finger ([Haegens et al., 2010](#); [Litvak et al., 2007](#); [Medvedovsky et al., 2007](#)). The stimuli were delivered with a constant current high voltage stimulator (Digitimer, Hertfordshire, UK). The intensity (350–600 mA, average 500 mA) of the 200 μ s electric pulses was set to a salient, yet comfortable level as individually established prior to the recordings. The task consisted of 200 trials lasting ~2.5 seconds each (ISI 2000-3000 ms, tactile stimulation 200 μ s, blink period every 7 trials for 2500 ms).

In the second task (visual task, ~12 min), subjects were visually stimulated with a foveal, circular sine wave grating ([Hoogenboom et al., 2006](#)). The sine wave grating contracted inward, toward the fixation point (diameter 5 deg, spatial frequency 2 cycles/deg, contrast 100%, velocity 1.6 deg/s, duration 1350 ms). The task consisted of 200 trials lasting ~3.5 seconds each (ISI 1500-2500 ms, visual stimulation 1350 ms, blink period every 10 trials 2500 ms).

In the third task (auditory task, ~6 min), brief tones (frequency 1000 Hz, duration 5 ms, ~70 dB SPL) were presented binaurally via MEG-compatible air tubes ([Todorovic](#)

[et al., 2011](#)). The task consisted of 250 trials lasting ~1 second each (ISI 1000-1250 ms, auditory stimulation 5 ms, blink period every 10 trials 2500 ms).

All tasks contained deviant trials (omission of a pulse in the tactile task, outward contracting sine wave gratings in the visual task, and 1050 Hz tones in the auditory task). Subjects were instructed to count the deviants to encourage them to remain engaged throughout the experiment and attending the stimuli in all three tasks. A simple query at the end of each task ('How many deviants did you count?') was used for a check. Subjects had a binomial choice; e.g. 'More than 30' or 'Less than 30', to be answered with a single button press with the right index finger (average accuracy was 75%). The stimuli were presented using a PC running Presentation software (Neurobehavioral Systems, Albany, CA, USA).

The stimuli used in the group MEG studies were comparable to those used in the single subject recordings described above; i.e. electrical pulses (97 ± 2.25 trials per subject; mean \pm SD) delivered to the left thumb at 150% threshold level in the first study ([Haegens et al., 2012](#)), a foveally presented circular sine wave grating that contracted toward the fixation point (2.7 cycles/deg; velocity, 0.75 deg/s; contrast 100%; 140 ± 23 trials) in the second study ([van Pelt et al., 2012](#)), and presentations of brief tones (20 ms; 1318 Hz; ~75 dB SPL; 150 trials) in the third study ([Todorovic and de Lange, 2012](#)).

2.4. Data acquisition

Ongoing brain activity was recorded using a whole-head magnetoencephalograph (MEG) with 275 axial gradiometers (VSM/CTF Systems, Port Coquitlam, British Columbia, Canada) in seated position (analog low-pass filter, 300 Hz; sampling rate, 1200 Hz). The subject's head position relative to the MEG sensors was measured before,

during, and after each session using localization coils, placed at anatomical fiducials (nasion, left and right ear canals). High-resolution anatomical images of the whole brain for forward model generation were acquired (voxel size = 1mm³) using a 1.5-T Siemens Avanto scanner (Erlangen, Germany). During MR acquisition, identical earplugs (now with a drop of Vitamin E in place of the MEG localization coils) were used for co-registration of the MRI and MEG data.

2.5. Online head repositioning

The CTF MEG system comes with three head localization coils, which are small coils that, when energized by an electrical current, result in a field distribution that approximates magnetic dipoles. Each coil is driven with sinusoidal current at a unique frequency and the combined field distribution is measured by the MEG channels. The contribution from each coil is extracted using spectral line extraction, and a magnetic dipole fit is performed on the extracted signals for each of the frequencies to determine the position of the corresponding coil. For each coil, the data contains the x-, y-, and z-coordinates in a 3-D cartesian coordinate system defined relative to the dewar.

The CTF MEG system also provides a shared memory interface in which the data is available for real-time analysis. Software from the open source FieldTrip toolbox ([Oostenveld et al., 2011](#)) transfers this data from shared memory to a FieldTrip buffer on the acquisition computer. The data in this FieldTrip buffer is read on another computer over a TCP connection, which gives it access to the real-time coordinates of the head localization coils. The implementation we used in the current study is specific for the CTF MEG system, but the real-time software interface has recently been implemented for Neuromag MEG systems as well ([Sudre et al., 2011](#)).

The subjects reposition their heads with the aid of a visual projection using a projector and a screen mounted in front of the subject. A 3-D figure is displayed with a target head position. The figure shows the positions of the localization coils from a previous recording session, together with the real-time position of the localization coils. The subject's instruction is to match the real-time localization coil positions with the target positions, by moving his head until the graphical markers are overlaying. The distance to the target location is color-coded to aid the subject (Animation S1). All online software is freely available as part of the FieldTrip toolbox (([Oostenveld et al., 2011](#)), see also <http://www.ru.nl/donders/fieldtrip>).

2.6. Data analysis

Data were analyzed offline using the FieldTrip toolbox and MATLAB (MathWorks, Natick, MA, USA). Trials with muscle and SQUID artifacts were removed from the MEG time-series using standardized procedures.

For the single subject analyses, this resulted in 90-100% (mean = 97%) of the original (non-deviant) trials being included for further analysis. The data was segmented around each stimulus presentation and baseline corrected using an interval of 100 ms before the occurrence of the stimulus. The analyses consisted of computing the somatosensory evoked fields (SEF; tactile task; 40-50 ms, ([Haegens et al., 2010](#); [Litvak et al., 2007](#); [Medvedovsky et al., 2007](#))), visually induced gamma-band activity (visual task; 0-500 ms, 65±10 Hz, ([Hoogenboom et al., 2006](#))) and auditory evoked fields (AEF; auditory task; 90-100 ms, ([Todorovic et al., 2011](#))).

The general sensor level analysis of the three tasks was performed by testing the SEF peak, visually induced gamma-band activity, and AEF peak against the activity in

prestimulus baseline using non-parametric cluster-based permutation paired samples t-tests ([Maris and Oostenveld, 2007](#)). For the SEF and AEF the baseline was selected from -100 to 0 ms. For the visually induced gamma-band activity the baseline was selected from -200 to 0 ms. Only the last 150 trials of each task were used for the analyses to ensure that signal-to-noise ratios, degrees of freedom, and adaptation effects were matched between sessions.

The source modeling of the median nerve SEF implicated fitting equivalent current dipoles models to the data using a single-shell volume conduction model of the brain ([Nolte, 2003](#)). This volume conduction model was co-registered to each subject's sensor locations; we chose to use the average location of the combined sessions' head positions at recording onsets. The consistency of the position of the fitted dipole in a pair of measurements was determined through bootstrapping (1000 repetitions) of the concatenated trials (150 from one session, 150 from another). We chose to describe the variance in dipole position by quantifying the volume of the 95% confidence ellipsoid. This volume is defined by computing the multivariate (3-dimensional) eigenvectors and their values to estimate the 95% confidence according to McIntyre and colleagues ([McIntyre et al., 1998](#)).

Sources of visually induced gamma-band activity were reconstructed using DICS, a frequency domain 'beamforming' approach ([Gross et al., 2001](#); [Van Veen et al., 1997](#)). This method constructs a spatial filter for each of the 3-dimensional grid positions covering the brain (10 mm spacing), which passes activity from each grid location with unit gain, while maximally suppressing activity from all other sources. The beamformer spatial filter is constructed from the lead field and the cross-spectral density matrix of the

data. The lead field is the physical forward model of the field distribution calculated from an assumed source at a given location and the subject-specific volume conduction model. The sessions were beamformed separately using session- and subject-specific lead fields and cross-spectral density matrices. The single-trial beamformer estimates of the two sessions were concatenated and their consistencies were evaluated by comparing the t-statistics (task vs. baseline activity) for dataset AC to that of dataset BD.

Sources of the AEFs were reconstructed using minimum-norm estimates. This method is a distributed inverse solution, constrained by a minimum-norm current estimate. The source space consisted of a large number of equivalent current dipoles placed on the cortical surface (preprocessed with the FreeSurfer and MNE Suite software packages, Martinos Center for Biomedical Imaging, Charlestown, MA, USA). It estimates the amplitude of all modeled source locations simultaneously and recovers a source distribution with minimum overall energy that produces data consistent with the measurement. This distributed source reconstruction was applied to each session before concatenation and subsequent statistical analyses (task vs. baseline activity).

With respect to the data obtained from the group MEG studies, we performed analyses similar to the general sensor level analyses described above. Separately for each study, single-subject statistical assessments were made and the peak activations (i.e. the absolute maximum of the subject t-statistics) were then tested against null at the group-level. The statistical assessments in the first study were made by comparing somatosensory evoked activity in the right hemisphere around 50-60 ms after stimulus onset (i.e. around the P60 trough), with activity in a 100 ms baseline period (97 ± 2.25 trials, mean \pm SD). For the second and third study respectively, comparisons were made

between gamma-band activity induced during a 600 ms task period and activity in 600 ms prestimulus baseline (140 ± 23 trials), and between auditory evoked activity around 90-100 ms (i.e. around the N1 peak) and activity in 100 ms prestimulus baseline (150 trials).

2.7. Testing the online head repositioning procedure

The circumcenter of the three head localization coils, i.e. the center of the circle that passes through all the positions of the fiducials, was used as an index for head position. Differences in head positions between sessions were obtained by computing the position of the head on a trial-by-trial basis of each session. Subsequently, a principal component analysis was used to project these 3-D positions on the axes that explain the most variance. To test for systematic differences in head positions, we computed the statistical difference in head positions between the two pairs of sessions (between sessions A and C and between B and D) using independent samples t-tests.

To test for changes in statistical sensitivity of the data due to online head repositioning (dataset AC vs. dataset BD), we compare the two pairs of measurements on their task-specific statistical assessments (see section 2.6) at the source level. The sensor level statistics are affected by the proximity of the head to the sensors ([Gaetz et al., 2008](#)). In the four sessions we did not explicitly control for this proximity, causing the measurement pairs AC and BD to have trivial differences in sensor level statistical values.

2.8. Testing the offline GLM-based head movement compensation

The continuous representation of the fiducial locations is written to disk along with the MEG by the acquisition software. Trial-by-trial estimates of the position and the orientation of the circumcenter of the three fiducial markers were computed. These were

demeaned and z-transformed to obtain the normalized deviants, i.e. translations ($\mathbf{H}_x, \mathbf{H}_y, \mathbf{H}_z$) and rotations ($\mathbf{H}_\varphi, \mathbf{H}_\theta, \mathbf{H}_\psi$), from the average head position and orientation. For both the sensor- and source level analyses, the data can be modeled with the following linear equation:

$$\mathbf{Y} = \mathbf{b}_0\mathbf{H}_0 + \mathbf{b}_1\mathbf{H}_x + \mathbf{b}_2\mathbf{H}_y + \mathbf{b}_3\mathbf{H}_z + \mathbf{b}_4\mathbf{H}_\varphi + \mathbf{b}_5\mathbf{H}_\theta + \mathbf{b}_6\mathbf{H}_\psi + \mathbf{E} \quad (8)$$

where \mathbf{Y} is a $1 \times K$ vector with the sensor- or source data over K trials, \mathbf{b}_0 is the intercept constant, \mathbf{H}_0 is a $1 \times K$ vector of ones, \mathbf{b}_{1-6} are regression coefficients for the head position and orientation, and \mathbf{E} is unexplained model error. The least squares solution to the linear equation,

$$\min ||\mathbf{Y} - \mathbf{bH}||^2 \quad (9)$$

results in a vector of \mathbf{b} values per channel/voxel for each session of each subject.

Subsequently, the estimated contributions of the regressors to the (source reconstructed) signal amplitude or spectral power can be removed from the original single-trial data:

$$\mathbf{Y}_{clean} = \mathbf{Y} - \mathbf{b}_{1..6}\mathbf{H}_{x..y} \quad (10)$$

where \mathbf{Y}_{clean} represents the data with the movement related variance removed. Note that this general linear modeling (GLM) approach only affects the signal variance and not the signal mean over trials; i.e. the intercept constant \mathbf{b}_0 remains in the data.

An important aspect in the practical application is that the compensation should be performed in conjunction with the statistical analysis and cannot be done at an arbitrary point in the analysis pipeline. E.g., in the case of ERFs, the estimation of the regression coefficients \mathbf{b} is performed separately for each channel and each latency, i.e. vector \mathbf{Y} is formed for each channel and for each latency and the regression coefficients \mathbf{b} are estimated for the specific channel and latency. In the case of powerspectra, the

estimated regression coefficients are channel and frequency specific, and in the case of time-frequency responses they are channel, latency and frequency specific. Consequently, after compensation, the sensor level data cannot be used anymore for source modeling. To employ the GLM based compensation on the source level, single trial estimates for the cortical locations of interest have to be made from the original sensor level data, preferably using a common spatial filter based on all trials. The beta weights are subsequently estimated for each cortical location and the variance in source amplitude over trials that is explained by the head movement is removed.

To account for the non-linear effects of head motion on the signal, we chose to consider also the squares, cubes and all their derivatives (the first three terms in the Taylor series expansion) of the head movement parameters in the model (resulting in a total of 36 regressors plus one constant). Following the removal of the trial-by-trial variance that was explained by the head movements, the task vs. baseline activation t-scores were computed and compared to the t-scores without the head movement compensation. We report descriptive statistics (t-score histograms and peak values) of the single subject analyses at the sensor and source level. Furthermore, we document how the GLM-based head movement compensation affects group level inferential statistics (second level effect sizes) by employing this technique on the single-subject data from the three group MEG studies.

3. Results

3.1. Online head repositioning

Subjects were consistently able to reposition their heads, effectively reducing intersession distances in head position at recording onsets; from 4.8 and 6.8 mm to 1.2 and 2.0 mm for subject *MN* and *LB* respectively (see Table 1). Visual inspection showed that the lack of repositioning resulted in session C to be an outlier (shown in green in Fig. 2), while the head positions during sessions A, B and D were closer to each other. It can also be observed from Fig. 2 that the subjects' heads, throughout the ~30 min. recordings, slowly but progressively drifted away.

Repositioning improved the consistencies of head positions in paired datasets as indicated by smaller statistical intersession difference in the positions; for subject *MN*, $t(1077) = -74$ with, and $t(1100) = -100$ without repositioning; for subject *LB*, $t(1155) = 19$ with, and $t(1151) = 351$ without repositioning. This improvement was most pronounced early after repositioning, i.e. during the tactile task; subject *MN*, $t(307) = -57$ with, and $t(330) = -180$ without repositioning; subject *LB*, $t(332) = 15$ with, and $t(343) = 314$ without repositioning.

Table 1. | Intersession Euclidean distances in head position of subjects *MN* and *LB*.

Sessions	Time	Distance (mm, t-value*)	
		Subject <i>MN</i>	Subject <i>LB</i>
A and C	Recording onset	4.8	6.8
(without repositioning, different day)	Tactile task (0-10 min)	5.4, t(330) = -180	7.1, t(343) = 314
	Visual task (11-22 min)	4.5, t(341) = -84	7.1, t(358) = 267
	Auditory task (23-28 min)	4.1, t(425) = -196	8.4, t(446) = 342
	Throughout recording	4.6, t(1100) = -100	7.5, t(1151) = 351
B and D	Recording onset	1.2	2.0
(with repositioning, different day)	Tactile task (0-10 min)	2.7, t(307) = -57	1.3, t(332) = 15
	Visual task (11-22 min)	4.3, t(332) = -109	2.0, t(357) = 4
	Auditory task (23-28 min)	6.2, t(434) = -215	4.9, t(462) = 103
	Throughout recording	4.6, t(1077) = -74	2.9, t(1155) = 19
A and B**	Recording onset	2.0	2.7
(with repositioning, same day)	Tactile task (0-10 min)	2.3, t(317) = 34	1.2, t(338) = 10
	Visual task (11-22 min)	3.8, t(339) = 33	2.2, t(363) = -5
	Auditory task (23-28 min)	6.3, t(425) = 214	3.9, t(458) = -82
	Throughout recording	4.3, t(1085) = 48	2.2, t(1163) = -14

* Statistical difference in position along the axis that explained most variance in both sessions combined (independent samples t-tests). All differences were statistically significant ($p < 0.05$).

** Shown for illustration purposes; i.e. subjects were consistently able to reposition their heads.

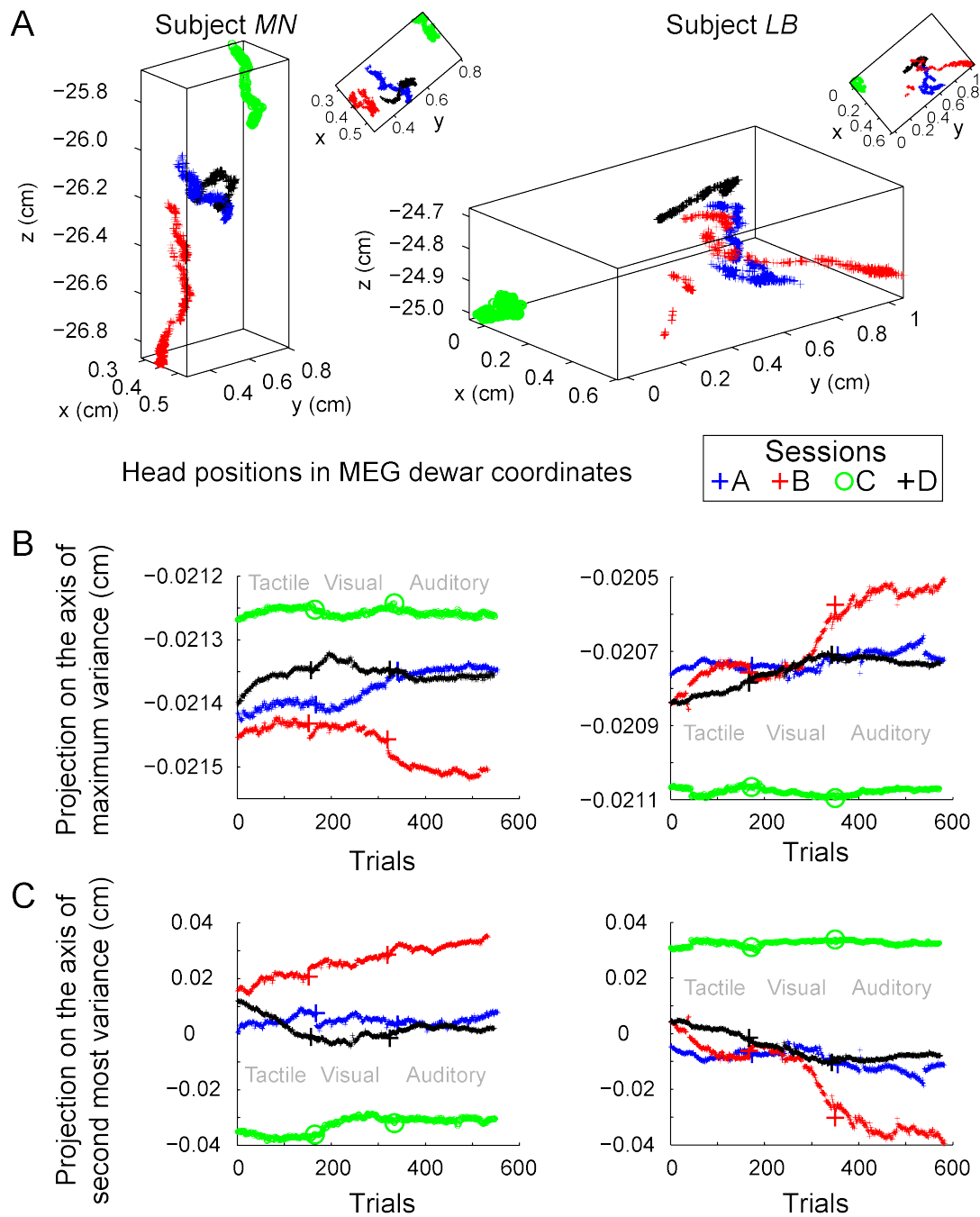


Fig. 2. Head positions, as indexed by the circumcentra of the three head localization coils, throughout the recording sessions of subjects *MN* (left panel) and *LB* (right panel). (A) Trial-to-trial head positions plotted in MEG dewar coordinates. (B) Head positions plotted along the axis explaining most variance in the head positions of all four sessions together against trials, where zero is recording onset and the respective tasks are denoted. (C) Same as in B, but plotted along the axis of second most variance.

We next investigated the consequences of repositioning on the source reconstructed data. For the median nerve somatosensory evoked fields (SEFs), repositioning of each subject reduced the variability in dipole fit positions (quantified by the 95% confidence ellipsoid volume) from 0.88 to 0.58 cm³ and from 0.18 to 0.14 cm³ respectively for both subjects *MN* and *LB* (see Fig. 3A; $-28 \pm 8\%$, mean \pm SD). Furthermore, it enhanced peak t-statistics of visually induced gamma-band activity from 11.9 to 14.0 and from 21.2 to 23.7 (see Fig. 3B; $15 \pm 4\%$), but not that of auditory evoked fields (AEFs) in the chronologically last task; from 17.3 to 17.2 and from 20.8 to 20.5 (see Fig. 3C; $-1 \pm 1\%$).

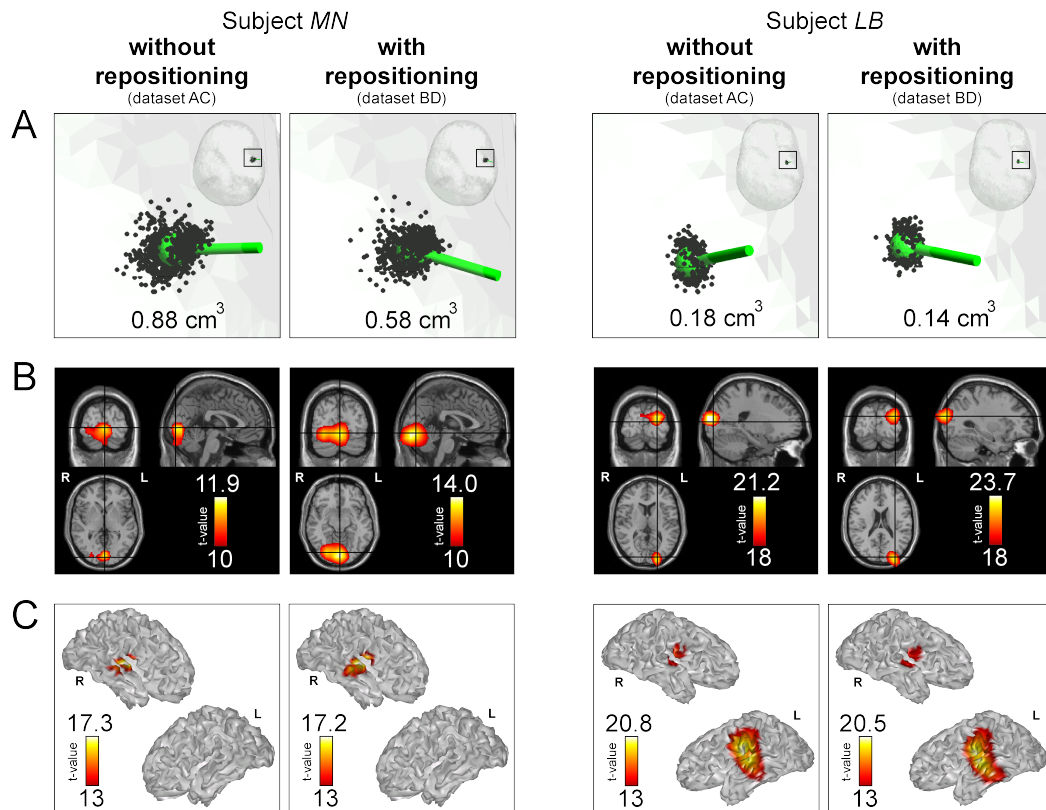


Fig. 3. Source level consequences of online head repositioning between sessions for subjects *MN* and *LB*. Panels follow the order of the experimental tasks. (A) Trials were randomly selected from concatenated SEF sessions, averaged and dipole fitted (1000 iterations). The variance in dipole position (black dots) of median nerve somatosensory evoked fields (40-50 ms) was described by quantifying the volume of the 95% confidence ellipsoid. The green marker represents the averaged dipole position and its orientation. (B) Source localization (beamforming) of visually-induced gamma-band activity (65 ± 10 Hz, 0-500 ms). The threshold of the color axis was raised in order to resolve the spatial structure around the statistically significant peaks. The upper t-values are the peaks. (C) Source localization (minimum-norm estimation) of auditory evoked fields (90-100 ms).

3.2. Offline general linear modeling

Head position and orientation confounds were estimated and their contribution was removed from the single-trial sensor- and source level data. Comparing peak t-statistics with and without this operation, we found GLM to yield improvements in all task vs. baseline activity contrasts of both subjects *MN* and *LB*, both for sensor- and source level (see Table 2, $9 \pm 3\%$ increase in peak t-statistics, overall mean \pm SD). Example topographic plots and histograms show that, with regression analysis, the distribution of t-statistics overall appears increased with the shape preserved (Fig 4.).

Table 2. | Combined single subjects results of the online and offline head movement compensation: repositioning and general linear modeling. The task effects are expressed in terms of consistency. At the source level; dipole position variance for the SEFs (the smaller, the more consistent) and peak t-values of visually induced gamma-band activity and AEFs (the larger, the more consistent). At the sensor level (*italic type*); peak t-values of the contrasts in each task (the larger, the more consistent).

Task	Subject	Without repositioning				With repositioning			
		Standard		GLM		Standard		GLM	
Tactile	<i>MN</i>	0.88 cm ³	<i>t 12.6</i>	n.a.	<i>t 13.2</i>	0.58 cm ³	<i>t 10.8</i>	n.a.	<i>t 11.5</i>
	<i>LB</i>	0.18 cm ³	<i>t 20.8</i>	n.a.	<i>t 23.1</i>	0.14 cm ³	<i>t 24.5</i>	n.a.	<i>t 27.0</i>
Visual	<i>MN</i>	<i>t 11.9</i>	<i>t 9.8</i>	<i>t 12.6</i>	<i>t 10.4</i>	<i>t 14.0</i>	<i>t 9.5</i>	<i>t 14.9</i>	<i>t 10.1</i>
	<i>LB</i>	<i>t 21.2</i>	<i>t 18.7</i>	<i>t 24.3</i>	<i>t 21.9</i>	<i>t 23.7</i>	<i>t 23.7</i>	<i>t 26.1</i>	<i>t 25.7</i>
Auditory	<i>MN</i>	<i>t 17.3</i>	<i>t 24.6</i>	<i>t 18.9</i>	<i>t 26.3</i>	<i>t 17.2</i>	<i>t 25.0</i>	<i>t 18.0</i>	<i>t 26.8</i>
	<i>LB</i>	<i>t 20.8</i>	<i>t 33.2</i>	<i>t 22.3</i>	<i>t 37.8</i>	<i>t 20.5</i>	<i>t 30.8</i>	<i>t 22.2</i>	<i>t 32.9</i>

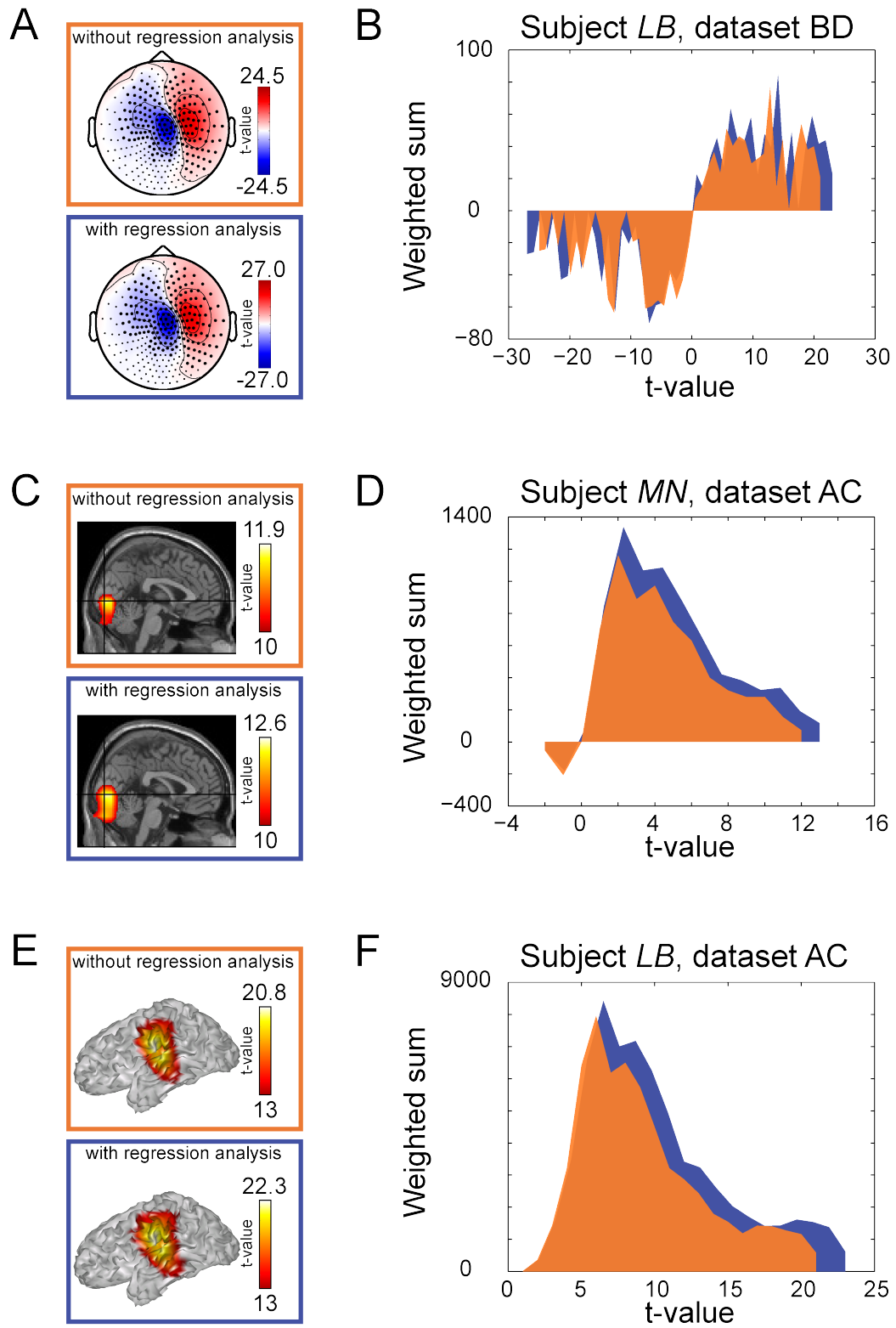


Fig. 4. Example statistical distributions with (blue) and without (orange) offline GLM-based head movement compensation. Each row displays one of the experimental tasks for one of the subjects. Note the different color scaling limits. (A) SEFs of subject *LB*, sessions B and D combined. Highlighted sensors indicate statistically significant differences ($p < 0.05$, corrected for multiple comparisons). (B) Histogram of the t-values of all channels and timepoints in the 40-50 ms interval, with (blue) and without (orange) regression analysis. Each histogram bin is weighted by its corresponding t-value. (C) Visually-induced gamma-band activity (65 ± 10 Hz, 0-500 ms) of subject *MN*, sessions A and C combined. (D) Histogram of the t-values of all voxels. (E) AEFs (90-100 ms) of subject *LB*, sessions A and C combined. (F) Histogram of the t-values of all cortical mesh surfaces.

Employing the GLM-based head movement compensation on sensor level data from three existing group studies revealed t-statistics that were greater than without using this technique. On average, peak t-statistics of activity evoked during 97 electrical pulses delivered to the left thumb improved by $23\% \pm 5\%$ in the first study (mean \pm SEM, 16 subjects mean; from $t(96) = 1.09$ to $t(96) = 1.39$, $p \ll 0.001$). In a similar vein, the effect size of the increase in peak t-statistics of induced gamma-band activity during 140 presentations of a circular sine wave grating in the second study was $29 \pm 4\%$ (32 subjects mean; from $t(139) = 13.4$ to $t(139) = 16.9$, $p \ll 0.001$). In the third study, head movement compensation yielded a $15 \pm 1\%$ increase in absolute peak t-statistics of activity evoked during 150 presentations of brief tones (20 subjects mean; from $t(149) = 3.61$ to $t(149) = 4.15$, $p \ll 0.001$).

4. Discussion

The present study investigated online and offline tools to compensate MEG data for head movement, as assessed through a statistical evaluation that is similar to how analysis is performed in most cognitive research projects. We recorded single subjects' brain activity in four sessions (Fig. 1) during the performance of three tasks (tactile, visual, auditory) to demonstrate the applicability of the investigated techniques to a wide range of tasks and experiments. We analyzed data from three larger MEG group studies to further validate the effect of the offline GLM-based technique on statistical sensitivity.

Using a real-time head localizer, subjects were consistently able to accurately reposition their heads between sessions. We observed that online head repositioning effectively reduced inter-session differences in head position (Fig. 2 and Table 1), thereby improving the statistical assessment of brain activity recorded during those sessions (Fig. 3). Interestingly, we observed this improvement also when we analyzed the recordings separately and combined them in source space (Fig. 3B). This finding suggests that in the combined analysis of two sessions, different head positions negatively affect the outcomes, even if accounted for by the source estimation. We hypothesize this to be due to differences in signal-to-noise ratio that are caused by differences in the distance between the sources and sensors, and due to the non-linear fitting of those sources.

Regression analyses, i.e. the offline incorporation of the head position time-series into a general linear model (GLM), successfully reduced the confounding variance that was due to within-sessions head movements. Our subjects did not make abrupt movements but slowly drifted down (see Fig. 2A and B), a movement that can be well compensated with offline general linear modeling (Fig. 4). The use of GLM to remove

confounding head motion is common practice in the analysis of functional magnetic resonance imaging ([Worsley and Friston, 1995](#)). To our knowledge the present study is the first demonstration that it can successfully be applied to MEG recordings. The application of the GLM-based approach to a 16 subject study addressing somatosensory spatial attention ([Haegens et al., 2012](#)) shows an improvement of statistical sensitivity, as assessed by an increase in t-scores, by 23%. The application of the same method to a 32 subject visual attention ([van Pelt et al., 2012](#)) and a 20 subject auditory expectation study ([Todorovic and de Lange, 2012](#)) demonstrated an increase in t-scores of 29% and 15% respectively. In each study the initial statistical sensitivity was already sufficient to address the research question for the respective studies and the improvement with the GLM method did not change the inferences that were drawn from the data. However, the large increase in statistical sensitivity suggests that the GLM method allows future studies to be performed with smaller subject group sizes, or alternatively allows studies to be performed with smaller effect sizes. Furthermore, by compensating for head movement related variance, this technique opens the way for cleaner investigations of trial-by-trial coupling of behavioral measures and the MEG signal.

The combination of both these online and offline tools yielded the largest improvement, i.e. online repositioning by means of a real-time head localizer reducing the between-sessions variance and offline GLM regressing out the within-sessions variance. The present study does not address the use of the real-time head localizer to reduce the variance within a session. We suggest that the real-time head localizer can also be used to compensate for within-sessions variance by correcting for head movement using a short repositioning instruction between experimental blocks. This could

counteract the slow but progressive drifting away from the position at recording onset of the subject's head without the need for head fixation. Such an approach may be specifically of relevance for studies that include subject groups that find it more difficult to maintain a constant position over a long period of time.

Finally, we have demonstrated that the tools introduced here can be readily applied to a wide range of tasks and experiments. Compared to the existing offline compensation methods which are based on sensor interpolation or lead field adjustments (see section 1) and for which an implementation is not available for all MEG systems, the application of these tools is relatively straightforward and is made available in the open-source FieldTrip toolbox, which allows it to be employed on data from all commonly used MEG systems. The user does not need detailed additional information (e.g. source and head model) and does not need to make modeling specific choices. It remains to be seen how the tools presented here complement and compare to the existing methods when dealing with the consequences of head movements on statistical sensitivity. For instance, the within-session head repositioning, as suggested in this paper, may have a positive effect on the SSS-based sensor level interpolation method ([Taulu et al., 2005](#)) by virtue of reducing trial-by-trial variations of head position and inherent improvements in signal-to-noise ratio. In a similar vein, it would be interesting to study how general linear modeling enhances statistical sensitivity after incorporation of head position information into the source reconstruction procedure ([Uutela et al., 2001](#)). The latter method, either by the relatively noise-sensitive adjustment of the lead field matrix on a trial-by-trial basis (see Eq. (4)) or using an averaged, spatially blurred version of the lead field (see Eq. (5) and (6)), has proven to reduce source localization error after head movement

([Uutela et al., 2001](#)). However, to date it has not been investigated whether and how it affects statistical sensitivity. The blurred version provides a static solution for the inverse source estimation and therefore cannot account for the dynamic trial-by-trial variation in the relative location of the sources (see supporting information for an initial exploration of this method on the present data). Consequently, it does not contribute to the statistical power, which we aimed at with the present study.

In summary, we consider the real-time head localizer tool a valuable addition to the experimental setup and the use of the GLM-based head movement compensation a necessary attribute of the MEG analysis toolbox.

Acknowledgements

The authors thank Stefan Klanke for contributing FieldTrip software to transfer data from the CTF shared memory to the FieldTrip buffer, Lennart Verhagen for assisting with the implementation of general linear modeling, Stan van Pelt and Saskia Haegens for contributing data, and Stephen Whitmarsh for fruitful discussions.

References

- Adjamian, P., Barnes, G.R., Hillebrand, A., Holliday, I.E., Singh, K.D., Furlong, P.L., Harrington, E., Barclay, C.W., Route, P.J., 2004. Co-registration of magnetoencephalography with magnetic resonance imaging using bite-bar-based fiducials and surface-matching. *Clin Neurophysiol* 115, 691-698.
- Dale, A.M., Sereno, M.I., 1993. Improved Localization of Cortical Activity by Combining Eeg and Meg with Mri Cortical Surface Reconstruction - a Linear-Approach. *Journal of Cognitive Neuroscience* 5, 162-176.
- de Munck, J.C., Verbunt, J.P., Van't Ent, D., Van Dijk, B.W., 2001. The use of an MEG device as 3D digitizer and motion monitoring system. *Phys Med Biol* 46, 2041-2052.
- Gaetz, W., Otsubo, H., Pang, E.W., 2008. Magnetoencephalography for clinical pediatrics: the effect of head positioning on measurement of somatosensory-evoked fields. *Clin Neurophysiol* 119, 1923-1933.
- Gross, J., Kujala, J., Hamalainen, M., Timmermann, L., Schnitzler, A., Salmelin, R., 2001. Dynamic imaging of coherent sources: Studying neural interactions in the human brain. *Proc Natl Acad Sci U S A* 98, 694-699.
- Haegens, S., Luther, L., Jensen, O., 2012. Somatosensory anticipatory alpha activity increases to suppress distracting input. *J Cogn Neurosci* 24, 677-685.
- Haegens, S., Osipova, D., Oostenveld, R., Jensen, O., 2010. Somatosensory working memory performance in humans depends on both engagement and disengagement of regions in a distributed network. *Hum Brain Mapp* 31, 26-35.
- Hamalainen, M.S., Ilmoniemi, R.J., 1994. Interpreting Magnetic-Fields of the Brain - Minimum Norm Estimates. *Medical & Biological Engineering & Computing* 32, 35-42.
- Heim, S., Amunts, K., Mohlberg, H., Wilms, M., Friederici, A.D., 2006. Head motion during overt language production in functional magnetic resonance imaging. *Neuroreport* 17, 579-582.

- Hoogenboom, N., Schoffelen, J.M., Oostenveld, R., Parkes, L.M., Fries, P., 2006. Localizing human visual gamma-band activity in frequency, time and space. *Neuroimage* 29, 764-773.
- Knosche, T.R., 2002. Transformation of whole-head MEG recordings between different sensor positions. *Biomed Tech (Berl)* 47, 59-62.
- Kominis, I.K., Kornack, T.W., Allred, J.C., Romalis, M.V., 2003. A subfemtotesla multichannel atomic magnetometer. *Nature* 422, 596-599.
- Litvak, V., Zeller, D., Oostenveld, R., Maris, E., Cohen, A., Schramm, A., Gentner, R., Zaaroor, M., Pratt, H., Classen, J., 2007. LTP-like changes induced by paired associative stimulation of the primary somatosensory cortex in humans: source analysis and associated changes in behaviour. *Eur J Neurosci* 25, 2862-2874.
- Maclaren, J., Herbst, M., Speck, O., Zaitsev, M., 2012. Prospective motion correction in brain imaging: A review. *Magn Reson Med*.
- Maris, E., Oostenveld, R., 2007. Nonparametric statistical testing of EEG- and MEG-data. *J Neurosci Methods* 164, 177-190.
- McIntyre, J., Stratta, F., Lacquaniti, F., 1998. Short-term memory for reaching to visual targets: psychophysical evidence for body-centered reference frames. *J Neurosci* 18, 8423-8435.
- Medvedovsky, M., Taulu, S., Bickmullina, R., Paetau, R., 2007. Artifact and head movement compensation in MEG. *Neurol Neurophysiol Neurosci*, 4.
- Nieuwenhuis, I.L., Takashima, A., Oostenveld, R., Fernandez, G., Jensen, O., 2008. Visual areas become less engaged in associative recall following memory stabilization. *Neuroimage* 40, 1319-1327.
- Nolte, G., 2003. The magnetic lead field theorem in the quasi-static approximation and its use for magnetoencephalography forward calculation in realistic volume conductors. *Phys Med Biol* 48, 3637-3652.

- Numminen, J., Ahlfors, S., Ilmoniemi, R., Montonen, J., Nenonen, J., 1995. Transformation of multichannel magnetocardiographic signals to standard grid form. *IEEE Trans Biomed Eng* 42, 72-78.
- Nurminen, J., Taulu, S., Okada, Y., 2008. Effects of sensor calibration, balancing and parametrization on the signal space separation method. *Phys Med Biol* 53, 1975-1987.
- Oostenveld, R., Fries, P., Maris, E., Schoffelen, J.M., 2011. FieldTrip: Open source software for advanced analysis of MEG, EEG, and invasive electrophysiological data. *Comput Intell Neurosci* 2011, 156869.
- Sander, T.H., Preusser, J., Mhaskar, R., Kitching, J., Trahms, L., Knappe, S., 2012. Magnetoencephalography with a chip-scale atomic magnetometer. *Biomed Opt Express* 3, 981-990.
- Singh, K.D., Holliday, I.E., Furlong, P.L., Harding, G.F., 1997. Evaluation of MRI-MEG/EEG co-registration strategies using Monte Carlo simulation. *Electroencephalogr Clin Neurophysiol* 102, 81-85.
- Sudre, G., Parkkonen, L., Bock, E., Baillet, S., Wang, W., Weber, D.J., 2011. rtMEG: a real-time software interface for magnetoencephalography. *Comput Intell Neurosci* 2011, 327953.
- Taulu, S., Simola, J., Kajola, M., 2005. Applications of the signal space separation method. *Ieee Transactions on Signal Processing* 53, 3359-3372.
- Thesen, S., Heid, O., Mueller, E., Schad, L.R., 2000. Prospective acquisition correction for head motion with image-based tracking for real-time fMRI. *Magn Reson Med* 44, 457-465.
- Todorovic, A., de Lange, F.P., 2012. Repetition suppression and expectation are dissociable in time in early auditory evoked fields. *J Neurosci* In press.

Todorovic, A., van Ede, F., Maris, E., de Lange, F.P., 2011. Prior expectation mediates neural adaptation to repeated sounds in the auditory cortex: an MEG study. *J Neurosci* 31, 9118-9123.

Uutela, K., Taulu, S., Hamalainen, M., 2001. Detecting and correcting for head movements in neuromagnetic measurements. *Neuroimage* 14, 1424-1431.

van Pelt, S., Boomsma, D.I., Fries, P., 2012. Magnetoencephalography in twins reveals a strong genetic determination of the peak frequency of visually induced gamma-band synchronization. *J Neurosci* 32, 3388-3392.

Van Veen, B.D., van Drongelen, W., Yuchtman, M., Suzuki, A., 1997. Localization of brain electrical activity via linearly constrained minimum variance spatial filtering. *IEEE Trans Biomed Eng* 44, 867-880.

Wehner, D.T., Hamalainen, M.S., Mody, M., Ahlfors, S.P., 2008. Head movements of children in MEG: quantification, effects on source estimation, and compensation. *Neuroimage* 40, 541-550.

Wilson, H.S., 2004. Continuous head-localization and data correction in a whole-cortex MEG sensor. *Neurol Clin Neurophysiol* 2004, 56.

Worsley, K.J., Friston, K.J., 1995. Analysis of fMRI time-series revisited--again. *Neuroimage* 2, 173-181.

Online and offline tools for head movement compensation in MEG

Arjen Stolk^a, Ana Todorovic^a, Jan-Mathijs Schoffelen^{a,b}, Robert Oostenveld^a

^aRadboud University Nijmegen, Donders Institute for Brain, Cognition and Behaviour;

^bMax Planck Institute for Psycholinguistics, Nijmegen, Netherlands

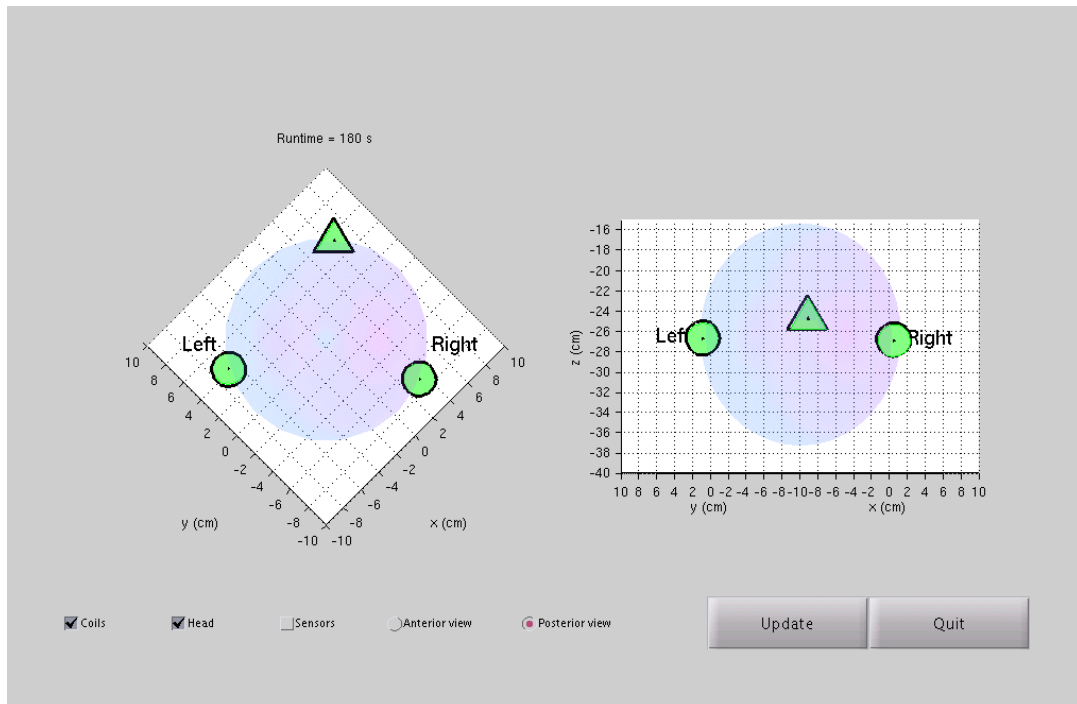
Forward calculation correction and statistical sensitivity

Forward calculation correction is a technique that incorporates the variability in head position into the forward calculations of the magnetic field (see Eq. (5) and (6)). For a dipole with an arbitrary location and orientation, the magnetic field picked up by a sensor coil at any position relative to the dipole can be computed. Variability in the exact location of the dipole relative to the sensor due to changes in head position can be taken into account by computing a linear combination of the modeled magnetic fields for different sensor locations. We took a similar approach as proposed by Uutela and colleagues ([Uutela et al., 2001](#)). For computational efficiency, rather than taking a plain average of the lead fields computed for each trial (and head position) separately, we computed a weighted average of a well-chosen set of lead fields. These sets of lead fields reflected a representative set of positions of the head relative to the sensors. We used k-means clustering on the single trial head position estimates and obtained 10 clusters. The centroid of each of these clusters was used as a head position for which the lead fields of the sources were computed. The numbers of trials contributing to each of the clusters were used as a weighting factor, with which the lead fields were weighted before they

were summed across the clusters. The lead fields obtained using this approach were used for the source reconstruction of activity evoked in all three tasks (see section 2.6) and the statistical sensitivity was compared to that without using this correction (listed under ‘Standard’ in Table 2).

The incorporation of variable head positions into the magnetic field forward calculations did not reduce the variance in dipole position of the SEFs, from 0.88 to 0.84 cm³ (‘dataset AC’) and from 0.58 to 0.60 cm³ (‘dataset BD’) for subject *MN* and from 0.18 to 0.22 cm³ and from 0.14 to 0.11 cm³ for subject *LB* ($0 \pm 18\%$, overall mean \pm SD). Furthermore, it did not significantly improve the peak t-statistics of beamformed visually induced gamma-band activity ($1 \pm 1\%$, overall mean \pm SD; subject *MN*: from $t = 11.9$ to 11.9 and from $t = 14.0$ to 14.0 ; subject *LB*: from $t = 21.2$ to 21.4 and from $t = 23.7$ to 23.9) and minimum-norm estimated AEFs ($1 \pm 3\%$, overall mean \pm SD; subject *MN*: from $t = 17.3$ to 17.4 and from $t = 17.2$ to 17.5 ; subject *LB*: from $t = 20.8$ to 20.1 and from $t = 20.5$ to 21.1).

The lack of this method contributing to the trial-by-trial consistency, and thus the statistical sensitivity of the data, can be explained: the varying head position during the recording gets represented in a spatially blurred version of the actually measured magnetic field and the lead fields used in the forward calculation. Although the blurred lead field can provide a more accurate spatial topography of the true sources and thereby improve the accuracy of the reconstructed source location, the static lead field solution cannot account for the dynamic trial-by-trial variability that is represented as across-trial variance of the source positions and source amplitudes.



Anim. S1. Screenshots of the real-time head localizer, captured during the recording of session B of subject *MN*. Repositioning of a subject can be performed by visualizing the anatomical fiducials from a reference dataset (nasion, left and right ear canals, black unfilled markers) and the graphically updating of the real-time head position. To aid the subject with repositioning, the real-time fiducial positions are color coded to indicate the distances to the targets (green < 1.5 mm, orange < 3 mm, and red > 3 mm).